Journal of Natural Science Review

Vol. 4, No. 1, 2026
https://kujnsr.com
e-ISSN: 3006-7804

A Novel, Cost-Effective Post-Doping Method to Produce Nitrogen-Doped Activated Carbon from Rice Husk for CO_2 Adsorption

Reza Joia✉[1], Abdulraouf Rashid[2], Naseer Mukhlis[3], Meiram Atamanov[4], Azizullah Usofi[3]

[1]Department of Chemistry, Education Faculty, Nimruz University, Nimruz, Afghanistan
[2] Department of Horticulture, Agriculture Faculty, Nimruz University, Nimruz, Afghanistan
[3] Department of Chemistry, Education Faculty, Bamyan University, Bamyan, Afghanistan
[4] Department of Chemical Physics and Material Science, Faculty of Chemistry and Chemical Technology, al-farabi Kazakh National University, Almaty, Kazakhstan
✉E-mail: nasariayaz@gmail.com (corresponding author)

ABSTRACT

Nitrogen-doped activated carbon (N-doped AC) from agricultural waste offers a low-cost route to solid sorbents for post-combustion CO_2 capture. However, there are limited straightforward and scalable methods for producing N-doped AC with a large surface area, high nitrogen content, and strong CO_2 adsorption. Thus, this study aims to synthesize rice husk-derived N-doped AC by optimizing the surface morphology and nitrogen functionality to enhance CO_2 capture efficiency and to quantify adsorption, correlating the gains with BET surface area and microporosity. Rice husk was carbonized via pyrrole-assisted pyrolysis at 450 ℃ for 45 min with a 90 min dwell, the carbonized rice husk was then activated chemically using a 4:1 ratio of KOH to carbonized rice husk, heated to 800℃ at a ramp rate of 15 ℃ per min under a flow of N_2 gas at 150 ml/min for 60 min, Subsequently, N-doping was performed by immersing the activated carbon in a urea solution with a mass ratio of 4:1 (urea solution to AC) at 600℃ for 60 min. The obtained N-doped AC exhibits a remarkable surface area of 2986.6 m²/g and a significantly enhanced CO_2 adsorption capacity of 6.5 mmol/g under ambient conditions. Incorporating approximately 6% nitrogen into the carbon structure optimizes its porosity and structural properties. The integrated carbonization, activation, and urea post-doping sequence provides a reproducible pathway to high-performance, waste-derived CO2 sorbents, highlighting rice husk as a viable feedstock and underscoring the synergistic roles of micro/mesoporosity and nitrogen functionalities in boosting physisorption-dominated CO_2 capture.

ARTICLE INFO

Article history:

Received: October 22, 2025
Revised: November 18, 2025
Accepted: February 10, 2026
Published: March 31, 2026

Keywords:

Chemical activation; CO_2 adsorption; N-doped AC; post-doping method; Rice husk

To cite this article: Joia, R., Mukhlis, N., Rashid, A., Atamanov M., & Usofi, A. (2026). Modelling and Forecasting Wholesale Potato Prices in Northern India Using SARIMA. *Journal of Natural Science Review, 4* (1), 78-92. https://doi.org/10.62810/jnsr.v4i1.335

Link to this article: https://kujnsr.com/JNSR/article/view/335

INTRODUCTION

Atmospheric carbon dioxide (CO_2) is the primary driver of current climate change, and alongside emission mitigation efforts (Jones et al., 2023), point-source capture remains an urgent priority (Martin-Roberts et al., 2021). Among capture routes, solid adsorption on

porous carbons is attractive because the sorbents are regenerable, composition-tunable (Bari & Jeong, 2023), and manufacturable from low-cost wastes (Z. Li et al., 2025). Activated carbon (AC) is a high-surface-area, micro/mesoporous material produced by carbonizing a precursor and activating it to open a network of pores (Joia, Atamanov, et al., 2024). When AC is doped with nitrogen, nitrogen atoms are introduced into the carbon lattice or grafted onto its surface; the resulting basic and polar sites can strengthen CO_2 surface interactions (Spessato et al., 2022). In this context, adsorption refers to CO_2 molecules adhering to internal surfaces (especially within ultramicropores <0.8 nm), as distinct from absorption into a bulk phase. "Post-doping" denotes introducing nitrogen after base AC has been formed, in contrast to in-situ co-doping during carbonization/activation. This study develops a novel, cost-effective post-doping method to produce nitrogen-doped activated carbon (N-doped AC) from rice husk for enhanced CO_2 adsorption.

The rationale is threefold. First, although nitrogen doping often increases CO_2 uptake, conventional routes can be costly, reagent-intensive, or harsh enough to collapse pores and reduce ultramicroporosity, which governs near-ambient adsorption (T. Li et al., 2023). Second, biomass sources differ widely; rice husk, an abundant, silica-rich residue generated at scale in rice-producing regions, offers a consistent, inexpensive feedstock and a clear circular-economy opportunity. Converting rice husk into high-value CO_2 sorbents reduces waste burdens while displacing petroleum-derived precursors (Chew et al., 2023). Third, post-doping separates texture generation from surface functionalization: producers can first manufacture a robust, texturally optimized AC and then tune nitrogen content in a subsequent, modular step. This decoupling can simplify scale-up, enable retrofits to existing AC lines, and allow precise control over nitrogen incorporation intensity (Karimi et al., 2023).

Despite these advantages, a persistent problem continues to limit deployment. Existing protocols often exhibit low nitrogen incorporation efficiency, defined here as the fraction of nitrogen precursor converted into stable nitrogen within the carbon while consuming significant energy or damaging microporosity (Geng et al., 2016). The literature lacks clear processing windows for rice-husk-derived AC that simultaneously (a) preserve or enrich ultramicropores and high accessible surface area, (b) introduce sufficient nitrogen to increase CO_2 affinity at 273–298 $°K$ and flue-gas-relevant partial pressures, and (c) keep consumables, energy, and cycle times low enough to be cost-competitive. This gap impedes techno-economic assessment and slows the translation of laboratory materials into practical sorbents.

Accordingly, the problem addressed here is how to design and optimize a post-doping strategy for rice-husk-derived AC that maximizes nitrogen incorporation efficiency and CO_2 uptake without sacrificing key textural attributes or inflating process cost. The overarching aim is to investigate and optimize post-doping processes, focusing on improving nitrogen incorporation efficiency and CO_2 uptake performance.

To achieve this aim, the study pursues two specific objectives:

1. Implement a novel post-doping method and systematically optimize parameters, including the amount of nitrogen precursor, treatment temperature, and time to maximize nitrogen incorporation while preserving or enhancing the microporous structure of the carbon material.
2. Quantify CO_2 adsorption under relevant temperatures and pressures and relate capacity gains to textural metrics (e.g., BET surface area and micropore volume) to identify the dominant drivers of performance.

These objectives motivate the following research questions and working hypotheses, framed within an empirical, optimization-oriented study. Can a scalable post-doping route be applied to a baseline rice-husk-activated carbon to increase near-ambient CO_2 uptake by maximizing nitrogen-incorporation efficiency while preserving or improving microporosity relative to the undoped baseline? We hypothesize that post-doped rice-husk AC will exhibit a statistically significant increase in CO_2 uptake relative to the baseline, without a decrease in micropore volume or a second. At near-ambient conditions, CO_2 capacity correlates more strongly with ultramicropore volume and specific N functionalities (pyridinic/graphitic fractions) than with total BET surface area or total nitrogen.

Scientifically, the study will clarify how post-doping parameters control nitrogen incorporation efficiency and the textural features that most strongly govern CO_2 uptake in rice-husk carbons. Practically, it aims to deliver a low-cost, modular protocol compatible with existing AC infrastructure and abundant agricultural waste. By aligning material performance with process simplicity, the work seeks to advance both understanding and scalability of waste-derived N-doped AC sorbents for CO_2 capture.

MATERIALS AND METHODS

Rice husk, a sustainable and cost-effective raw material, was obtained from local agricultural sources and used as the precursor for activated carbon synthesis due to its high carbon content, inherent porosity, and low ash levels (Menya et al., 2018). Ensuring sustainable sourcing and compatibility with activation methods enhances its efficiency and quality, guiding the preparation of high-quality N-doped activated carbon for optimal adsorption properties (Kundu et al., 2024). Before use, the rice husk was cleaned to remove extraneous materials and mixed plant straw, thoroughly washed three times with distilled water, and dried at room temperature for two days. The dried material was ground in a grinder and sieved to obtain particles of 100 µm (Figure 1).

Potassium hydroxide (KOH, ≥85% purity, Merck, Germany) was employed as the chemical activating agent, while urea (≥99% purity, Sigma-Aldrich, USA) served as the nitrogen source for post-doping. All chemicals were of analytical grade and used without further purification. Deionized water was used throughout all experimental procedures.

Preparation of Activated Carbon

The carbonization process began by heating 80 g of ground rice husk in an iron reactor at 450 ℃ for 45 min, followed by 90 min at the same temperature before cooling (Figure 1). The carbonized material was then transferred to a washing step, where sodium hydroxide was used to decompose lignin and hemicellulose and to remove impurities. This process also formed soluble salts or hydroxides, ensuring effective separation of undesirable compounds. This procedure was continued until the solution reached a neutral pH, after which the material was washed with distilled water and dried for three days.

The activation step involved mixing 20 g of the carbonized material (1/4 mass ratio) with 80 g of KOH, which was finely ground before processing. The mixture was heated in an iron reactor to 800 ℃ over 80 min at a controlled heating rate of 10 ℃/min. The material was held at 800 ℃ for 60 min, then cooled to 300 ℃ for 180 min. The reactor was removed and allowed to cool naturally, ensuring that the material stabilized at ambient temperature. A continuous flow of nitrogen gas at 150 mL/min was maintained throughout the activation phase for consistency (Figure 1). After activation, the material was thoroughly washed with distilled water and agitated until the pH reached neutral. Higher temperatures accelerate the reaction between KOH and the carbon matrix, forming K_2CO_3 and leading to further reactions in the carbon matrix (equation 1). At temperatures above 800 ℃, the potassium vapor expands the network, while the CO_2 and H_2O reactions etch the carbon structure and enhance pore formation (equation 2-5). At 900 ℃, mesopore formation increases, but causes erosion of the carbon matrix and reduced efficiency. Optimizing the balance between micro- and mesopores improves supercapacitor performance and CO_2 adsorption capacity.

$$6KOH + 2C \longrightarrow 2K + 3H_2 + 2K_2CO_3 \quad (1)$$

Reduction of KOH by carbon produces metallic K, hydrogen gas, and potassium carbonate. Metallic K intercalates into the carbon lattice, expanding pores.

$$2KOH \longrightarrow K_2O + H_2O \quad (2)$$

Thermal decomposition of KOH at high temperature.

$$C + H_2O \longrightarrow CO + H_2 \quad (3)$$

Steam gasification of carbon contributes to pore formation.

$$K_2CO_3 \longrightarrow K_2O + CO_2 \quad (4)$$

Decomposition of potassium carbonate releases CO_2 gas.

$$CO_2 + \mathrm{C} \longrightarrow CO \quad (5)$$

CO_2 reacts with carbon, further etching the matrix and generating additional porosity.

Nitrogen Doping Procedure

After the activation step, the nitrogen doping process was carried out using the post-doping method by mixing the urea-carbon solution in a 1 AC:4 urea:3 KOH ratio. The process began by preparing the urea solution, ensuring homogeneous distribution before adding carbon, and stirring for 24 h to facilitate nitrogen replacement. Ultrasound treatment enhanced molecular interactions and created a uniform doping environment prior to 4 hours of thermal

doping at 200 ℃ (Figure 1). The material was then brought to neutral pH using distilled water and a magnetic stirrer to stabilize its chemical composition. Finally, air drying at ambient temperature preserved the integrity of the doped material for further applications.

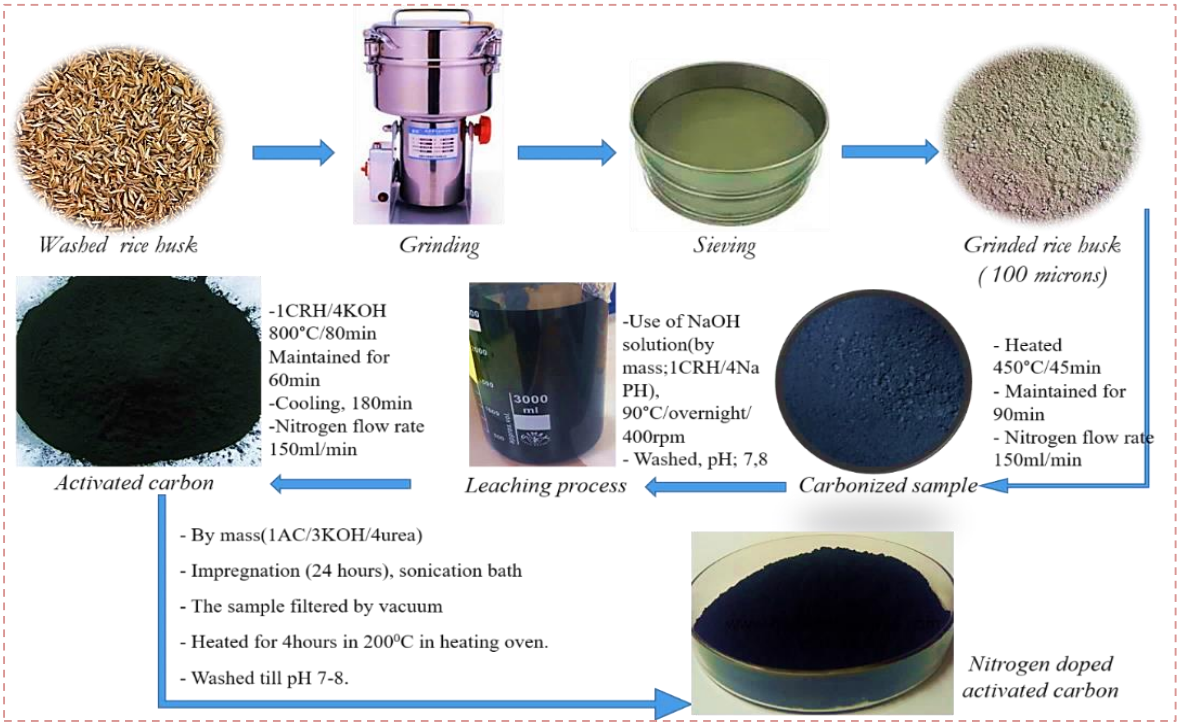

***Figure 1**. The sample preparation, carbonization, activation, and nitrogen doping steps in the production of N-doped AC*

FINDINGS

A variety of characterization techniques, including Brunauer–Emmett–Teller (BET) surface area analysis, X-ray diffraction (XRD), scanning electron microscopy (SEM), and Fourier transform infrared spectroscopy (FTIR), were employed to examine the structural, chemical, and surface properties of the N-doped activated carbon samples.

The specific surface areas of AC and N-doped were determined by the BET method using N_2 adsorption–desorption isotherms at 77.3 $°K$ after vacuum degassing to remove surface contaminants. BET surface area was calculated from the linear region of the isotherm (P/P_0 = 0.04–0.30), while pore volume and pore size distribution were obtained using H-K and NLDFT models. N-doped AC exhibited a higher surface area and micropore volume than pristine AC, attributed to nitrogen doping, which promotes pore development and generates additional surface defects and active sites. The enhanced surface area increases the number of accessible adsorption sites. At the same time, nitrogen functionalities improve surface polarity and adsorbate–adsorbent interactions (electrostatic attraction, hydrogen bonding, and π–π interactions), resulting in superior adsorption performance of N-doped AC (Table 1).

Table 1. *Show the surface area and porosity of activated carbon and nitrogen-doped activated carbon*.

AC		**Nitrogen-doped AC**	
S BET	2019.5 m^2/g	S BET	2986.6 m^2/g
Langmuir specific surface area	3194.9 m^2/g	Langmuir specific surface area	4065.5 m^2/g
Micropore volume (≤2.03 nm)	0.8 ml/g	Micropore volume (≤2.07 nm)	1.08 ml/g
Total pore volume of (≤2.54 nm)	0.9 ml/g	Total pore volume of (≤2.54 nm)	1.3 ml/g
Pore Size (Original) Median Pore Width	0.9 nm	Pore Size (Original) Median Pore Width	0.9 nm
Micropore Volume (P/P_0=0.127)	0.7 ml/g	Micropore Volume (P/P_0=0.119)	0.9 ml/g

By comparing the surface area and porosity of activated carbon and N-doped AC, we clearly see that post-doping strongly affects porosity and surface area, and this method demonstrates its effectiveness for nitrogen doping of activated carbon. And also according to nitrogen adsorption isotherms (Figure 2), we can see that the doping process strongly increases the adsorption capacity of activated carbon.

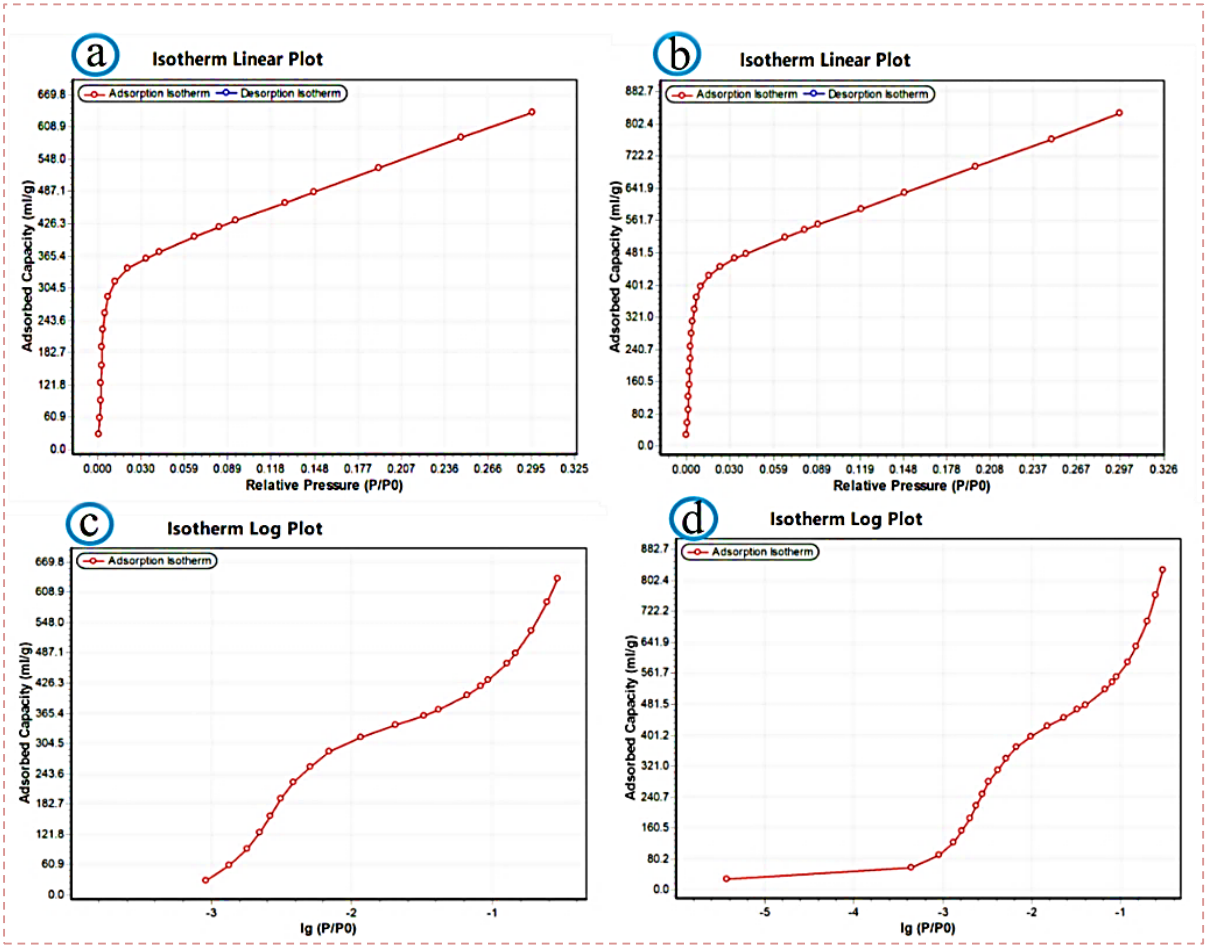

Figure 2. *The adsorption isotherm of activated carbon with N_2. And c) is its log plot, b) Show the adsorption isotherm of N-doped AC with N2 and d) is the log format plot*

To determine the micromorphology of the carbonized and N-doped material, scanning electron microscopy (SEM) was performed (Figure 3). The carbonized rice husk exhibited an irregular and compact morphology with limited porosity (Figure 3a). After KOH activation, the activated carbon (AC) exhibited a smoother, more uniform surface with numerous newly formed pores, confirming the effectiveness of the activation process (Figure 3b). In comparison, nitrogen-doped activated carbon (N-AC) displayed a more developed porous structure characterized by abundant micropores and slit-like openings (Figure 3c). Elemental mapping further confirmed the uniform distribution of carbon and nitrogen in N-AC (Figure 3d), indicating successful nitrogen incorporation. Overall, N-AC exhibited superior structural development compared to both carbonized rice husk and pristine AC, which is expected to enhance its adsorption performance.

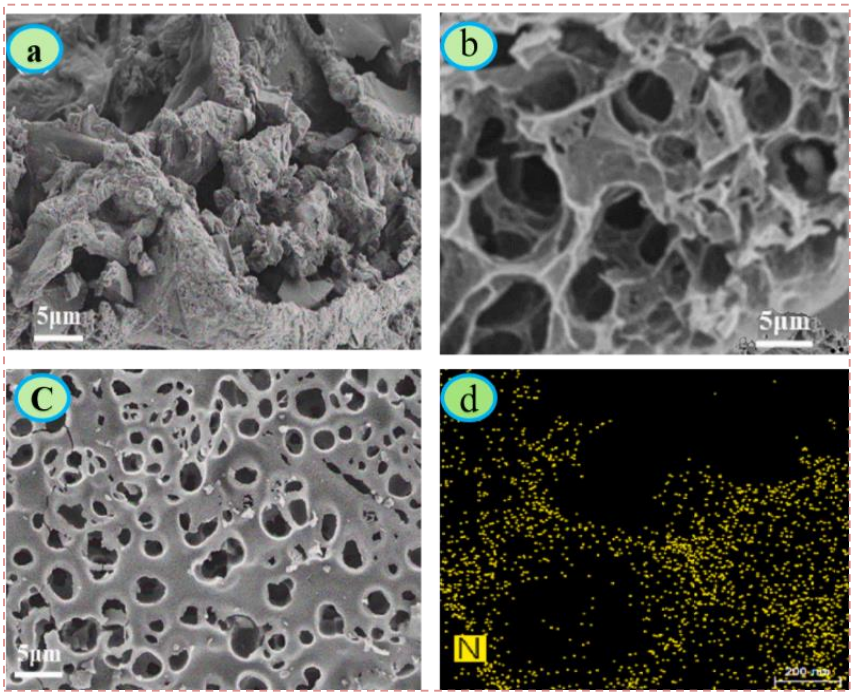

Figure 3. *The SEM images. a) SEM image of carbonized rice husk, b) SEM image of AC achieved from rice husk, c) SEM image of N-doped AC, d) Elemental mapping for nitrogen atoms in the structure of N-doped AC*

The X-ray diffraction (XRD) pattern shown in (Figure 4a and b); depicts the structural differences between the simple activated carbon and the nitrogen-doped ones. In (Figure 4a), which signs of simple activated carbon, the peak at 44 degrees is a little smaller than in (Figure 4b), the nitrogen-doped sample. This contradictory shows that the doping makes the (100) crystal plane more numerous in the porous carbon's crystalline structure. The X-ray diffraction discloses details about the atoms' positions in the crystalline lattice of the material. Pockets in the XRD pattern are the crystal planes that are the specific lattice in the crystal. Thus, in this instance, the representation of peaks at around 2θ = 25 and 44 degrees is due to the diffraction of the (002) and (100) crystal planes of graphitic carbon, respectively.

The (002) plane depicts the stacking of graphene layers within the crystal lattice; on the other hand, the (100) plane depicts the outline of the carbon atoms in each layer. Through the analysis of the variation or magnitude of these peaks in the XRD pattern, one can

determine the changes in the percentages or arrangements of these crystal planes. Within the experiment, the larger peak at 44 degrees in the nitrogen-doped sample indicates a greater alignment of the (100) crystal plane than in the simple activated carbon. This change in the crystalline structure implies that the atoms within the porous carbon have been rearranged by nitrogen doping, which can be used to improve the material's properties for certain applications.

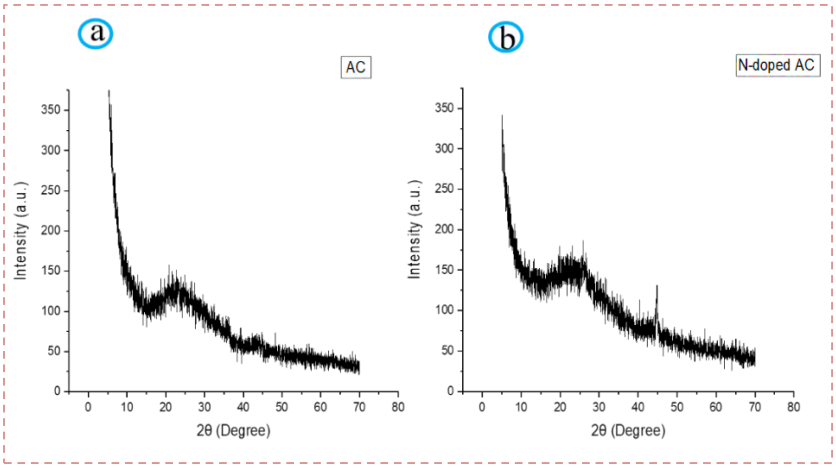

Figure 4. a *XRD pattern of activated carbon. b) N-doped AC*

Based on the FTIR analysis (Figure 5), several nitrogen functionalities were identified in the N-doped AC. The strong C–N stretching vibrations observed at 1099, 1040, and 1086 cm^{-1} indicate the presence of amine or aliphatic C–N groups (Alabadi et al., 2016). The absorption bands in the 1300–1600 cm^{-1} region are attributed to pyridinic nitrogen, amide groups, and C=N (imine-type or graphitic-related) nitrogen species. Vibrations occurring between 2800-3000cm-1 indicate the presence of -CH- bonds or alkyl groups within the activated carbon structure, Furthermore, the broad peaks at 3200–3450 cm^{-1} correspond to N–H stretching vibrations, confirming the existence of pyrrolic type nitrogen (Guo et al., 2024). Overall, the FTIR analysis suggests that nitrogen is incorporated mainly as pyridinic-N, Amide-N, C–N (amine-type), and C=N-related nitrogen species within the N-doped AC framework.

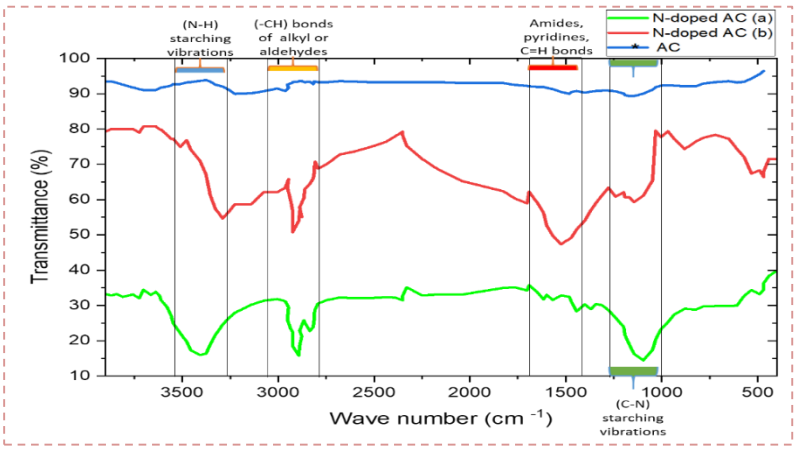

Figure 5. *Illustration of FTIR analysis results for determination of various functional groups vibration area of nitrogen doped samples and activated carbon*

Co2 Adsorption Performance

N-doped AC shows remarkable improvements in CO_2 adsorption due to its special properties. The nitrogen functional groups enhance chemical bonding with CO_2 molecules, boosting adsorption efficiency. This functionalization raises surface heterogeneity, creating more active sites and improving selectivity. Nitrogen doping also reshapes the pore structure, expanding surface area and pore volume for better CO_2 accommodation. The increased porosity allows more CO_2 to settle on the surface and deep inside the pores, maximizing adsorption capacity (Ding et al., 2016). Enhanced thermal stability makes nitrogen-doped carbon ideal for high-temperature CO_2 capture applications. A larger surface area offers more active adsorption sites, strengthening interactions between CO_2 molecules and the carbon surface. This broad surface also promotes faster CO_2 diffusion into the porous network, optimizing adsorption performance (Alabadi et al., 2020). N-doped AC is a strong candidate for CO2 capture and storage. Its unique blend of chemical functionalization, porosity, heterogeneity, and stability delivers outstanding CO_2 capture capabilities. The combination of nitrogen doping and large surface area ensures highly efficient CO_2 adsorption. Continued research into this material could push forward carbon capture technologies and help reduce greenhouse gas emissions (Taurbekov et al., 2023).

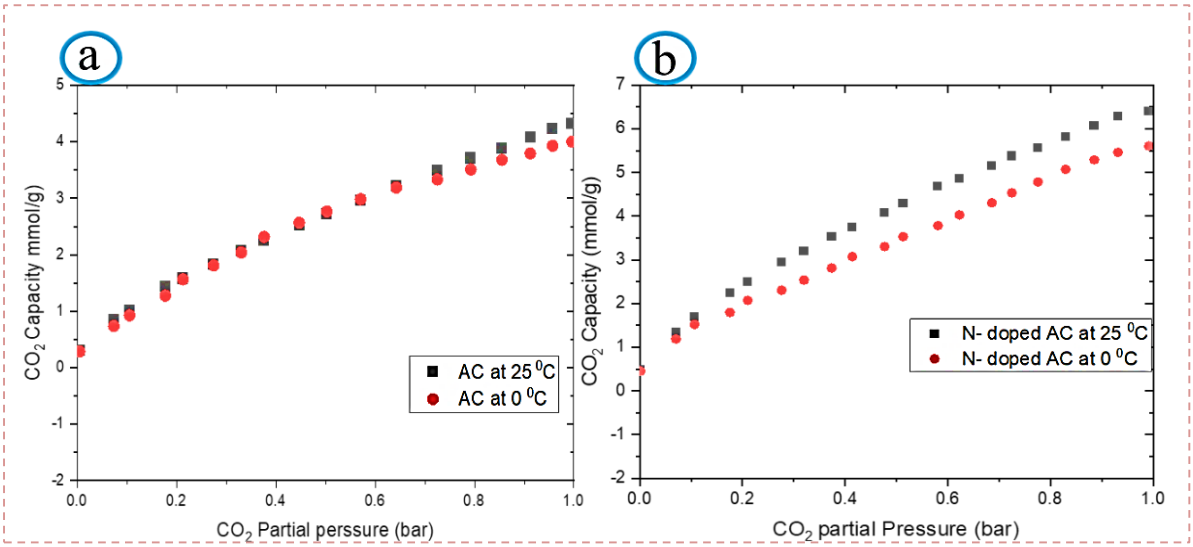

Figure 6. *Presents the CO_2 adsorption isotherms of activated carbon and N-doped AC. a) exhibit the CO_2 adsorption isotherms for simple activated carbon from rice husk at 273 °K and 298 °K. b) Show the CO_2 adsorption capacity for N-doped AC at 273 °K and 298 °K*

(Figure 6a and b); depict the CO_2 adsorption isotherms of two distinct samples: simple activated carbon, and N-doped AC made from rice husk. The isotherm plots show the differences that are not so easily seen between the two materials. (Figure 6a) shows that the simple activated carbon has an adsorption capacity of 4.5mmol/g at 1 bar pressure. But, in (Figure 6b), the N-doped AC proves that the adsorption capacity is so much higher, the adsorption capacity is increase from 4.5 mmol/g to 6.5 mmol/g.

The drastic improvement in the adsorption capacity that is proved by this research is a clear proof of the great influence that the doping process has on the porosity of the activated

carbon. The insertion of nitrogen into the carbon matrix not only modifies its structural characteristics but also opens up new ways for CO_2 to be adsorbed. The damage is caused by different physical and chemical interactions of the CO_2 molecules with the nitrogen atoms that are doped in the crystalline structure of activated carbon.

DISCUSSION

Nitrogen post-doping significantly enhanced the textural properties of activated carbon, increasing the BET surface area from 2019.5 $m^2\ g^{-1}$ (AC) to 2986.6 $m^2\ g^{-1}$ (N-doped AC) (~47.9%), accompanied by notable increases in micropore (+35%) and total pore volumes (+44.4%). Correspondingly, the CO_2 adsorption capacity at 1 bar increase from 4.5 mmol g^{-1} for AC to 6.5 mmol g^{-1} for N-doped AC (~44.4%). The close proportionality between the increases in micropore volume and CO_2 uptake indicates that adsorption is primarily governed by the development of accessible microporous surface rather than macroscopic morphological changes. This behavior agrees well with previous reports demonstrating that microporosity, particularly ultramicropores, dominates CO_2 physisorption at near-ambient conditions (Sai Bhargava Reddy et al., 2021), (Sevilla & Fuertes, 2011).

A more rigorous evaluation using surface area normalized uptake reveals nearly identical values (~2.23 mmol per 1000 m^2 for AC versus ~2.18 mmol per 1000 m^2 for N-doped AC), suggesting that nitrogen doping does not substantially alter adsorption efficiency on a per-area basis. However, when normalized to micropore volume, CO_2 capture increases from 5.63 to 6.02 mmol mL^{-1} (~7%), indicating improved utilization of micropores in N-doped AC. This enhancement is attributed to the formation of additional ultramicropores (<0.7 nm), which provide stronger adsorption potentials through overlapping van der Waals fields and are known to be particularly effective for CO_2 capture at 273–298 $°K$ and ≤1 bar. The nearly unchanged median pore width (~0.9 nm) supports the notion that nitrogen doping redistributes pores within the micropore regime rather than shifting average pore size, a phenomenon commonly associated with improved CO_2 capacity (Sevilla et al., 2013).

SEM analysis further corroborates these findings. The carbonized rice husk exhibits an irregular and relatively dense morphology with limited porosity, explaining its poor adsorption performance. After KOH activation, AC develops a smoother surface with abundant pores, greatly enhancing surface accessibility and adsorption sites. Upon nitrogen doping, N-doped AC displays a more highly developed porous structure with interconnected micropores and slit-like openings, facilitating faster diffusion and improved CO_2 accommodation. These morphological transformations directly contribute to the superior adsorption capacity of N-doped AC by providing both increased pore connectivity and greater exposure of internal adsorption surfaces (Sánchez-Sánchez et al., 2014).

FTIR analysis confirms successful nitrogen incorporation into the carbon framework in the form of pyridinic-N, pyrrolic-N, Graphitic-N, C–N (amine-type), and C=N–related functionalities (Figure 7). These nitrogen configurations collectively enhance CO_2 capture by increasing surface basicity, polarity, and electronic density, thereby strengthening

quadrupole–dipole and acid–base interactions between CO_2 molecules and the carbon surface (Wood & O'Hayre, 2014). Pyridinic nitrogen, located at the edges of graphene layers, provides strong Lewis basic sites and lone-pair electrons that interact effectively with acidic CO_2, significantly improving adsorption capacity (Ye et al., 2024). Pyrrolic nitrogen, incorporated within five-membered rings, contributes to surface polarity and overall basicity, further promoting CO_2 uptake (Liu et al., 2025). Graphitic nitrogen, embedded within the graphene lattice, enhances π-electron distribution and structural stability, indirectly benefiting CO_2 adsorption by improving electronic properties and adsorption-site accessibility (Shibuya et al., 2022). Although physical adsorption governed by microporosity remains the dominant mechanism, these chemically active nitrogen functionalities provide additional adsorption affinity, acting synergistically with the developed pore structure to yield the enhanced CO_2 performance observed for N-doped AC (L. Li et al., 2016)

Despite the observed enhancements, this study presents certain limitations. The experiments were performed under controlled laboratory conditions (273–298 K, ≤1 bar), which may not fully replicate the complex operational environments encountered in industrial CO_2 capture. Moreover, the long-term stability, regeneration performance, and scalability of the N-doped activated carbon were not assessed. Future investigations should prioritize evaluating the material under realistic flue gas conditions, examining alternative nitrogen doping strategies to optimize functional group distribution, and assessing the cyclic adsorption–desorption behavior to establish its potential for sustainable and large-scale CO_2 capture applications.

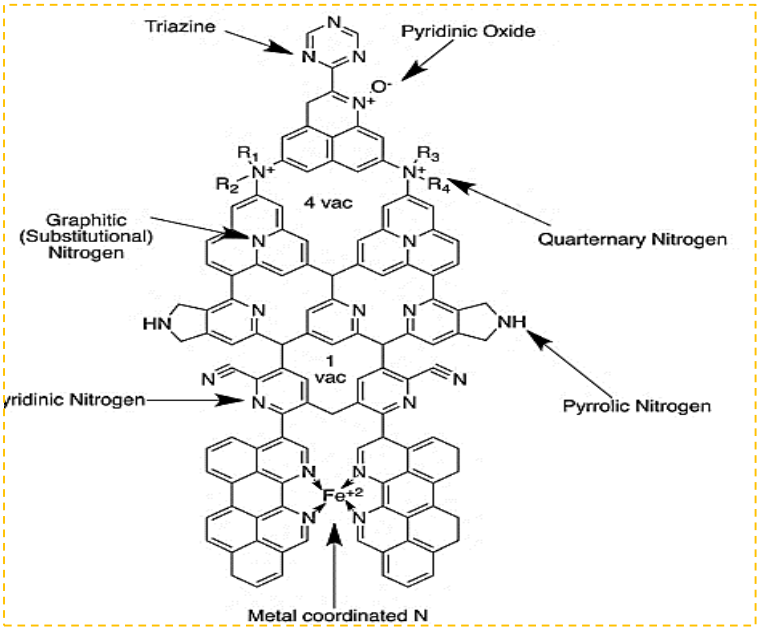

Figure 7. *Show the different type of nitrogen atoms in the structure of N-doped AC, Reproduced by permission (Wood & O'Hayre, 2014)*

CONCLUSION

This study reports the successful synthesis of N-doped AC through a novel post-doping method, resulting in a material with significantly enhanced CO_2 adsorption performance. SEM analysis highlighted distinct morphological differences: raw rice husk exhibited a compact, irregular structure; AC developed increased porosity and smoother surfaces following KOH activation; and N-doped AC showed a highly developed microporous network with slit-like openings, providing greater accessibility to adsorption sites. BET analysis confirmed a significant enhancement in surface area, from 2019.5 m^2/g for AC to 2986.6 m^2/g for N-doped AC, along with expanded micropore and total pore volumes, directly supporting higher CO_2 capture efficiency. FTIR characterization revealed the presence of nitrogen functional groups, including pyridinic-N, amine-N, and C=N species, which act as Lewis base sites to strengthen chemical interactions with CO_2. The combination of enhanced textural properties and nitrogen functionalities explains the superior CO_2 adsorption capacity of N-doped AC (6.5 mmol/g) relative to AC and raw rice husk. Future research should aim to optimize synthesis strategies and explore alternative nitrogen-doping approaches to improve material quality and scalability. Such advances could position N-doped AC as a key material for CO_2 capture and sustainable environmental technologies, representing a significant step toward a greener future.

AUTHOR'S CONTRIBUTIONS

- Reza Joia and Meiram Atamenov conceptualized and supervised the study.
- Naseer Mukhlis, Abdulraouf Rashid, and Azizullah Usofi collected the row data.
- Reza Joia analyzed the data and wrote the manuscript with input from all authors.
- All authors reviewed and approved the final version.

FUNDING INFORMATION

The authors declare that no funds, grants, or other support were received during the preparation of this manuscript.

CONFLICT OF INTEREST STATEMENT

The authors declare that there is no conflict of interest regarding the publication of this paper.

DATA AVAILABILITY

The data that support the findings of this study are available from the corresponding author upon reasonable request.

REFERENCE

Alabadi, A., a Abbood, H., & Dawood, A. (2020). Ultrahigh-CO 2 Adsorption Capacity and CO 2 /N 2 Selectivity by Nitrogen-Doped Porous Activated Carbon Monolith. *Bulletin of the Chemical Society of Japan*. https://doi.org/10.1246/bcsj.20190336

Alabadi, A., Abbood, H. A., Li, Q., Jing, N., & Tan, B. (2016). Imine-Linked Polymer Based Nitrogen-Doped Porous Activated Carbon for Efficient and Selective CO(2) Capture. *Scientific Reports*, *6*, 38614. https://doi.org/10.1038/srep38614

Bari, G. A. K. M. R., & Jeong, J.-H. (2023). Porous Carbon for CO2 Capture Technology: Unveiling Fundamentals and Innovations. *Surfaces*, *6*(3), 316–340. https://doi.org/10.3390/surfaces6030023

Chew, T. W., H'Ng, P. S., Luqman Chuah Abdullah, B. C. T. G., Chin, K. L., Lee, C. L., Mohd Nor Hafizuddin, B. M. S., & TaungMai, L. (2023). A Review of Bio-Based Activated Carbon Properties Produced from Different Activating Chemicals during Chemicals Activation Process on Biomass and Its Potential for Malaysia. *Materials*, *16*(23). https://doi.org/10.3390/ma16237365

Ding, S., Dong, Q., Hu, J., Xiao, W., Liu, X., Liao, L., & Zhang, N. (2016). Enhanced selective adsorption of CO2 on nitrogen-doped porous carbon monoliths derived from IRMOF-3. *Chem. Commun.*, *52*(63), 9757–9760. https://doi.org/10.1039/C6CC04416F

Geng, Z., Xiao, Q., Lv, H., Li, B., Wu, H., Lu, Y., & Zhang, C. (2016). One-Step Synthesis of Microporous Carbon Monoliths Derived from Biomass with High Nitrogen Doping Content for Highly Selective CO2 Capture. *Scientific Reports*, *6*(1), 30049. https://doi.org/10.1038/srep30049

Guo, T., Zhang, Y., Chen, J., Liu, W., Geng, Y., Bedane, A. H., & Du, Y. (2024). Investigation of CO2 adsorption on nitrogen-doped activated carbon based on porous structure and surface acid-base sites. *Case Studies in Thermal Engineering*, *53*, 103925. https://doi.org/https://doi.org/10.1016/j.csite.2023.103925

Joia, R., Atamanov, M., Umbetkaliev, K., Mohammadi, M. H., Sarwari, S. R., & Modaqeq, T. (2024). Exploring the versatile production techniques and applications of nitrogen-doped activated carbon. *Thermal Science and Engineering*, *7*(1), 5842. https://doi.org/10.24294/tse.v7i1.5842

Jones, M. W., Peters, G. P., Gasser, T., Andrew, R. M., Schwingshackl, C., Gütschow, J., Houghton, R. A., Friedlingstein, P., Pongratz, J., & Le Quéré, C. (2023). National contributions to climate change due to historical emissions of carbon dioxide, methane, and nitrous oxide since 1850. *Scientific Data*, *10*(1), 155. https://doi.org/10.1038/s41597-023-02041-1

Karimi, M., Shirzad, M., Silva, J. A. C., & Rodrigues, A. E. (2023). Carbon dioxide separation and capture by adsorption: a review. *Environmental Chemistry Letters*, 1–44. https://doi.org/10.1007/s10311-023-01589-z

Kundu, S., Khandaker, T., Anik, M. A.-A. M., Hasan, M. K., Dhar, P. K., Dutta, S. K., Latif, M. A., & Hossain, M. S. (2024). A comprehensive review of enhanced CO2 capture using activated carbon derived from biomass feedstock. *RSC Adv.*, *14*(40), 29693–29736. https://doi.org/10.1039/D4RA04537H

Li, L., Wang, Y., Gu, X., Yang, Q., & Zhao, X. (2016). Increasing the CO2 /N2 Selectivity with a Higher Surface Density of Pyridinic Lewis Basic Sites in Porous Carbon Derived from a Pyridyl-Ligand-Based Metal-Organic Framework. *Chemistry, an Asian Journal*, *11*(13), 1913–1920. https://doi.org/10.1002/asia.201600427

Li, T., An, X., & Fu, D. (2023). Review on Nitrogen-Doped Porous Carbon Materials for CO2 Adsorption and Separation: Recent Advances and Outlook. *Energy & Fuels*, *37*(12), 8160–8179. https://doi.org/10.1021/acs.energyfuels.3c00941

Li, Z., Feng, S., Yang, X., Lyu, H., Wei, S., & Shen, B. (2025). A review of biomass porous carbon for carbon dioxide adsorption from flue gas: Physicochemical properties and performance. *Fuel*, *387*, 134318. https://doi.org/https://doi.org/10.1016/j.fuel.2025.134318

Liu, B., Wang, Z., Zhou, L., Wang, T., Zhang, L., Ma, W., Fu, Q., & Chen, X. (2025). Pyridinic and pyrrolic nitrogen-doped porous carbon improves control of N2 and H2 adsorption thermodynamic for N2/H2 separation. *International Journal of Hydrogen Energy*, *122*, 107–116. https://doi.org/10.1016/j.ijhydene.2025.03.328

Martin-Roberts, E., Scott, V., Flude, S., Johnson, G., Haszeldine, R. S., & Gilfillan, S. (2021). Carbon capture and storage at the end of a lost decade. *One Earth*, *4*(11), 1569–1584. https://doi.org/https://doi.org/10.1016/j.oneear.2021.10.002

Menya, E., Olupot, P. W., Storz, H., Lubwama, M., & Kiros, Y. (2018). Production and performance of activated carbon from rice husks for removal of natural organic matter from water: A review. *Chemical Engineering Research and Design*, *129*, 271–296. https://doi.org/https://doi.org/10.1016/j.cherd.2017.11.008

Sai Bhargava Reddy, M., Ponnamma, D., Sadasivuni, K. K., Kumar, B., & Abdullah, A. M. (2021). Carbon dioxide adsorption based on porous materials. *RSC Advances*, *11*(21), 12658–12681. https://doi.org/10.1039/dora10902a

Sánchez-Sánchez, Á., Suárez-García, F., Martínez-Alonso, A., & Tascón, J. M. D. (2014). Influence of Porous Texture and Surface Chemistry on the CO2 Adsorption Capacity of Porous Carbons: Acidic and Basic Site Interactions. *ACS Applied Materials & Interfaces*, *6*(23), 21237–21247. https://doi.org/10.1021/am506176e

Sevilla, M., & Fuertes, A. B. (2011). Sustainable porous carbons with a superior performance for CO2 capture. *Energy Environ. Sci.*, *4*(5), 1765–1771. https://doi.org/10.1039/C0EE00784F

Sevilla, M., Parra, J. B., & Fuertes, A. B. (2013). Assessment of the role of micropore size and N-doping in CO2 capture by porous carbons. *ACS Applied Materials & Interfaces*, *5*(13), 6360–6368. https://doi.org/10.1021/am401423b

Shibuya, R., Takeyasu, K., Guo, D., Kondo, T., & Nakamura, J. (2022). Chemisorption of CO2 on Nitrogen-Doped Graphitic Carbons. *Langmuir*, *38*(47), 14430–14438. https://doi.org/10.1021/acs.langmuir.2c01987

Spessato, L., Duarte, V. A., Fonseca, J. M., Arroyo, P. A., & Almeida, V. C. (2022). Nitrogen-doped activated carbons with high performances for CO2 adsorption. *Journal of CO2 Utilization*, *61*, 102013. https://doi.org/10.1016/J.JCOU.2022.102013

Taurbekov, A., Abdisattar, A., Atamanov, M., Kaidar, B., Yeleuov, M., Joia, R., Amrousse, R., & Atamanova, T. (2023). Investigations of Activated Carbon from Different Natural Sources for Preparation of Binder-Free Few-Walled CNTs / Activated Carbon Electrodes. *Journal of Composites Science*, *7*(453), 1–12. https://doi.org/https://doi.org/10.3390/jcs7110452

Wood, K., & O'Hayre, R. (2014). Recent progress on nitrogen/carbon structures designed for use in energy and sustainability applications. *Energy & Environmental Science*, *7*. https://doi.org/10.1039/c3ee44078h

Ye, D., Leung, K. C., Niu, W., Duan, M., Li, J., Ho, P.-L., Szalay, D., Wu, T.-S., Soo, Y.-L., Wu, S., & Tsang, S. C. E. (2024). Active nitrogen sites on nitrogen doped carbon for highly efficient associative ammonia decomposition. *IScience*, *27*(8), 110571. https://doi.org/10.1016/j.isci.2024.110571